Unusual Structural Types in Manganese Cluster Chemistry from the Use of N , N , N ‘, N ‘-Tetrakis(2-hydroxyethyl)ethylenediamine: Mn 8 , Mn 12 , and Mn 20 Clusters

ARTICLE *in* INORGANIC CHEMISTRY · FEBRUARY 2008

Impact Factor: 4.76 · DOI: 10.1021/ic701971d · Source: PubMed

3 AUTHORS, INCLUDING:

Khalil Abboud
University of Florida
582 PUBLICATIONS **12,688** CITATIONS
SEE PROFILE

George Christou
University of Florida
758 PUBLICATIONS **29,583** CITATIONS
SEE PROFILE

Inorg. Chem. **2008**, *47*, 621–631

Unusual Structural Types in Manganese Cluster Chemistry from the Use of *N*,*N*,*N*′,*N*′-Tetrakis(2-hydroxyethyl)ethylenediamine: Mn_8, Mn_{12}, and Mn_{20} Clusters

Rashmi Bagai, Khalil A. Abboud, and George Christou*

Department of Chemistry, University of Florida, Gainesville, Florida 32611-7200

Received October 5, 2007

The syntheses, crystal structures, and magnetochemical characterization are reported for three new mixed-valent Mn clusters $[Mn_8O_3(OH)(OMe)(O_2CPh)_7(edte)(edteH_2)](O_2CPh)$ (**1**), $[Mn_{12}O_4(OH)_2(edte)_4Cl_6(H_2O)_2]$ (**2**), and $[Mn_{20}O_8(OH)_4(O_2CMe)_6(edte)_6](ClO_4)_2$ (**3**) ($edteH_4$ = $(HOCH_2CH_2)_2NCH_2CH_2N(CH_2CH_2OH)_2$ = *N*,*N*,*N*′,*N*′-tetrakis-(2-hydroxyethyl)ethylenediamine). The reaction of $edteH_4$ with $Mn(O_2CPh)_2$, $MnCl_2$, or $Mn(O_2CMe)_2$ gives **1**, **2**, and **3**, respectively, which all possess unprecedented core topologies. The core of **1** comprises two edge-sharing $[Mn_4O_4]$ cubanes connected to an additional Mn ion by a μ_3-OH^- ion and two alkoxide arms of $edteH_2^{2-}$. The core of **2** consists of a $[Mn_{12}(\mu_4\text{-}O)_4]^{24+}$ unit with S_4 symmetry. The core of **3** consists of six fused $[Mn_4O_4]$ cubanes in a 3 × 2 arrangement and linked to three additional Mn atoms at both ends. Variable-temperature, solid-state dc and ac magnetization (*M*) studies were carried out on complexes **1**–**3** in the 5.0–300 K range. Fitting of the obtained $M/N\mu_B$ vs H/T data by matrix diagonalization and including only axial zero-field splitting (ZFS) gave ground-state spin (*S*) and axial ZFS parameter (*D*) of $S = 8$, $D = -0.30$ cm^{-1} for **1**, $S = 7$, $D = -0.16$ cm^{-1} for **2**, and $S = 8$, $D = -0.16$ cm^{-1} for **3**. The combined work demonstrates that four hydroxyethyl arms on an ethylenediamine backbone can generate novel Mn structural types not accessible with other alcohol-based ligands.

Introduction

Interest in the preparation of polynuclear Mn complexes has developed worldwide for both fundamental scientific and technological reasons since the discovery that some of these molecules can behave as zero-dimensional nanoscale magnets now called single-molecule magnets (SMMs).[1] These are individual molecules that possess a significant barrier (vs *kT*) to magnetization relaxation and thus exhibit the ability to function as magnets below their blocking temperatures (T_B). The first SMM to be studied was $[Mn_{12}O_{12}(O_2CMe)_{16}(H_2O)_4]$,[2] and since then many polynuclear clusters containing 3d transition metals have been reported to be SMMs,[3] the vast majority of them being Mn complexes.[4] This is because Mn clusters often display relatively large ground-state *S*

* To whom correspondence should be adddressed. E-mail: christou@chem.ufl.edu. Tel.: +1-352-392-8314. Fax: +1-352-392-8757.

(1) (a) Christou, G.; Gatteschi, D.; Hendrickson, D. N.; Sessoli, R. *MRS Bull.* **2000**, *25*, 66. (b) Aromi, G.; Brechin, E. K. *Struct. Bonding* **2006**, *122*, 1. (c) Gatteschi, D.; Sessoli, R. *Angew. Chem., Int. Ed.* **2003**, *42*, 268. (d) Bircher, R.; Chaboussant, G.; Dobe, C.; Gudel, H. U.; Ochsenbein, S. T.; Sieber, A.; Waldmann, O. *Adv. Funct. Mater.* **2006**, *16*, 209.

(2) (a) Sessoli, R.; Gatteschi, D.; Caneschi, A.; Novak, M. A. *Nature* **1993**, *365*, 141. (b) Sessoli, R.; Tsai, H. L.; Schake, A. R.; Wang, S. Y.; Vincent, J. B.; Folting, K.; Gatteschi, D.; Christou, G.; Hendrickson, D. N. *J. Am. Chem. Soc.* **1993**, *115*, 1804.

(3) (a) Gatteschi, D.; Sessoli, R.; Cornia, A. *Chem. Commun.* **2000**, 725. (b) Sun, Z. M.; Grant, C. M.; Castro, S. L.; Hendrickson, D. N.; Christou, G. *Chem. Commun.* **1998**, 721. (c) Yang, E. C.; Hendrickson, D. N.; Wernsdorfer, W.; Nakano, M.; Zakharov, L. N.; Sommer, R. D.; Rheingold, A. L.; Ledezma-Gairaud, M.; Christou, G. *J. Appl. Phys.* **2002**, *91*, 7382. (d) Andres, H.; Basler, R.; Blake, A. J.; Cadiou, C.; Chaboussant, G.; Grant, C. M.; Gudel, H. U.; Murrie, M.; Parsons, S.; Paulsen, C.; Semadini, F.; Villar, V.; Wernsdorfer, W.; Winpenny, R. E. P. *Chem.—Eur. J.* **2002**, *8*, 4867. (e) Murugesu, M.; Mishra, A.; Wernsdorfer, W.; Abboud, K. A.; Christou, G. *Polyhedron* **2006**, *25*, 613.

(4) (a) Christou, G. *Polyhedron* **2005**, *24*, 2065. (b) Brechin, E. K. *Chem. Commun.* **2005**, 5141. (c) Aubin, S. M. J.; Wemple, M. W.; Adams, D. M.; Tsai, H. L.; Christou, G.; Hendrickson, D. N. *J. Am. Chem. Soc.* **1996**, *118*, 7746. (d) Dendrinou-Samara, C.; Alexiou, M.; Zaleski, C. M.; Kampf, J. W.; Kirk, M. L.; Kessissoglou, D. P.; Pecoraro, V. L. *Angew. Chem., Int. Ed.* **2003**, *42*, 3763. (e) Milios, C. J.; Raptopoulou, C. P.; Terzis, A.; Lloret, F.; Vicente, R.; Perlepes, S. P.; Escuer, A. *Angew. Chem., Int. Ed.* **2004**, *43*, 210. (f) Miyasaka, H.; Clerac, R.; Wernsdorfer, W.; Lecren, L.; Bonhomme, C.; Sugiura, K.; Yamashita, M. *Angew. Chem., Int. Ed.* **2004**, *43*, 2801. (g) Boudalis, A. K.; Donnadieu, B.; Nastopoulos, V.; Clemente-Juan, J. M.; Mari, A.; Sanakis, Y.; Tuchagues, J. P.; Perlepes, S. P. *Angew. Chem., Int. Ed.* **2004**, *43*, 2266. (h) Oshio, H.; Hoshino, N.; Ito, T.; Nakano, M. *J. Am. Chem. Soc.* **2004**, *126*, 8805.

10.1021/ic701971d CCC: $40.75
Published on Web 12/28/2007

Scheme 1

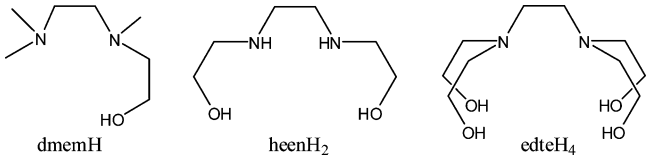

values, as well as negative *D* values (easy-axis anisotropy) associated with the presence of Jahn−Teller distorted Mn^{III} atoms.[5]

For the above reasons and more, there is a continuing search for new synthetic methods that can yield new polynuclear Mn/O clusters. In the design of a potentially new synthetic route to a polynuclear cluster, the choice of the ligands and bridging groups is vital. As part of our continuing search for such new methods, we have recently begun exploring the use of chelating/bridging groups based on the ethylenediamine backbone. We recently reported, for example, the use of dmemH and $heenH_2$ (Scheme 1) as new and flexible N,N,O and O,N,N,O chelates, respectively, for the synthesis of Fe_3, Fe_6, Fe_7, Fe_9, and Fe_{18} complexes, some of which possess novel Fe_x topologies.[6] The hydroxyethyl arms, on deprotonation, usually act as bridging groups and thus foster the formation of a high-nuclearity product. In the present work, we have extended this study by exploring the use in Mn cluster chemistry of the related, potentially hexadentate ligand *N*,*N*′,*N*′,*N*′-tetrakis(2-hydroxyethyl)ethylenediamine ($edteH_4$; Scheme 1). The $edteH_4$ molecule now provides four hydroxyethyl arms on an ethylenediamine backbone, and was considered an attractive potential new route to high-nuclearity products. Previous use of $edteH_4$ in the literature with other metals has been limited to the preparation of only mononuclear Ca and dinuclear Ba, Cu, and V complexes.[7] We herein report that the use of $edteH_4$ in a variety of reactions with Mn reagents has yielded novel Mn_8, Mn_{12}, and Mn_{20} complexes with core structures that are distinctly different from any seen previously. The syntheses, structures, and magnetochemical properties of these complexes will be described.

Experimental Section

Syntheses. All preparations were performed under aerobic conditions using reagents and solvents as received. $[Mn_3O(O_2CPh)_6(py)_2H_2O]$ (py = pyridine) was synthesized as reported elsewhere.[8]

$[Mn_8O_3(OH)(OMe)(O_2CPh)_7(edte)(edteH_2)](O_2CPh)$ (1). Method A. To a stirred solution of $edteH_4$ (0.05 g, 0.21 mmol) in CH_2Cl_2/MeOH (16/4 mL) was added $[Mn_3O(O_2CPh)_6(py)_2H_2O]$ (0.23 g, 0.21 mmol). The mixture was stirred for 30 min and filtered, and the filtrate was layered with Et_2O. X-ray-quality dark orange-brown crystals of **1**·$2CH_2Cl_2$·MeOH slowly formed over a week. They were collected by filtration, washed with Et_2O, and dried in vacuo. The yield was 40%. Dried solid appeared to be hygroscopic, analyzing as the dihydrate. Anal. Calcd (Found) for **1**·$2H_2O$ ($C_{77}H_{90}N_4Mn_8O_{31}$): C, 46.08 (45.97); H, 4.52 (4.36); N, 2.79 (2.81). Selected IR data (cm^{-1}): 2868(w), 1649(w), 1595(m), 1547(m), 1447(w), 1383(s), 1315(m), 1174(w), 1122(w), 1066(m), 911(w), 719(m), 676(w), 603(m), 536(m).

Method B. To a stirred solution of $edteH_4$ (0.10 g, 0.42 mmol) in MeCN/MeOH (10/5 mL) was added NEt_3 (0.18 mL, 1.28 mmol) followed by $Mn(O_2CPh)_2$ (0.42 g, 1.26 mmol). The resulting mixture was stirred for 1 h and filtered, and the filtrate was layered with Et_2O. Dark orange-brown crystals of **1** slowly formed over 5 days and were then isolated as in Method A. The yield was 20%. The product was identified by IR spectral comparison with material from Method A and elemental analysis. Anal. Calcd (Found) for **1**·$2H_2O$ ($C_{77}H_{90}N_4Mn_8O_{31}$): C, 46.08 (45.79); H, 4.52 (4.37); N, 2.79 (2.76).

$[Mn_{12}O_4(OH)_2(edte)_4Cl_6(H_2O)_2]$ (2). To a stirred solution of $edteH_4$ (0.15 g, 0.64 mmol) in MeCN/MeOH (10/1 mL) was added NEt_3 (0.09 mL, 0.64 mmol) followed by $MnCl_2$·$4H_2O$ (0.25 g, 1.26 mmol). The solution was stirred for 2 h and then filtered, and the brown filtrate was left undisturbed to evaporate slowly, giving X-ray-quality crystals of **2**·6MeCN·$^1/_2H_2O$ over 5 days. These were collected by filtration, washed with MeCN, and dried in vacuo. The yield was 25%. Dried solid analyzed as solvent-free. Anal. Calcd (Found) for **2** ($C_{40}H_{86}N_8Mn_{12}O_{24}Cl_6$): C, 24.83 (24.57); H, 4.48 (4.50); N, 5.79 (6.20); Cl, 10.99 (11.89). Selected IR data (cm^{-1}): 2854(m), 1631(w), 1465(w), 1359(w), 1270(w), 1160(w), 1088(s), 1059(s), 926(m), 899(m), 741(w), 669(m), 619(m), 557(m).

$[Mn_{20}O_8(OH)_4(O_2CMe)_6(edte)_6](ClO_4)_2$ (3). To a stirred solution of $edteH_4$ (0.10 g, 0.42 mmol) in MeOH (12 mL) was added NEt_3 (0.12 mL, 0.85 mmol) followed by $Mn(O_2CMe)_2$·$4H_2O$(0.21 g, 0.86 mmol) and then $NaClO_4$ (0.05 g, 0.41 mmol). The mixture was stirred for 1 h and filtered, and the filtrate was layered with Et_2O. X-ray-quality dark orange-brown crystals of **3**·10MeOH slowly formed over a week. They were collected by filtration, washed with a little Et_2O, and dried in vacuo. The yield was 20%. Dried solid appeared to be hygroscopic, analyzing as the pentahydrate. Anal. Calcd (Found) for **3**·$5H_2O$ ($C_{72}H_{152}N_{12}Mn_{20}O_{61}Cl_2$): C, 25.96 (25.92); H, 4.60 (4.69); N, 5.04 (4.54). Selected IR data (cm^{-1}): 2929(w), 1560(s), 1418(s), 1145(m), 1112(m), 1088(s), 910(m), 627(s), 563(m).

X-ray Crystallography. Data were collected on a Siemens SMART PLATFORM equipped with a CCD area detector and a graphite monochromator utilizing Mo Kα radiation ($\lambda = 0.71073$ Å). Suitable crystals of **1**·$2CH_2Cl_2$·MeOH, **2**·6MeCN·$^1/_2H_2O$, and **3**·10MeOH were attached to glass fibers using silicone grease and transferred to a goniostat where they were cooled to 173 K for data collection. Cell parameters were refined using up to 8192

(5) (a) Stamatatos, T. C.; Abboud, K. A.; Wernsdorfer, W.; Christou, G. *Angew. Chem., Int. Ed.* **2006**, *45*, 4134. (b) Stamatatos, T. C.; Abboud, K. A.; Wernsdorfer, W.; Christou, G. *Angew. Chem., Int. Ed.* **2007**, *46*, 884. (c) Milios, C. J.; Vinslava, A.; Wernsdorfer, W.; Prescimone, A.; Wood, P. A.; Parsons, S.; Perlepes, S. P.; Christou, G.; Brechin, E. K. *J. Am. Chem. Soc.* **2007**, *129*, 6547. (d) Ako, A. M.; Hewitt, I. J.; Mereacre, V.; Clerac, R.; Wernsdorfer, W.; Anson, C. E.; Powell, A. K. *Angew. Chem., Int. Ed.* **2006**, *45*, 4926. (e) Murugesu, M.; Habrych, M.; Wernsdorfer, W.; Abboud, K. A.; Christou, G. *J. Am. Chem. Soc.* **2004**, *126*, 4766. (f) Stamatatos, T. C.; Foguet-Albiol, D.; Masello, A.; Stoumpos, C. C.; Raptopoulou, C. P.; Terzis, A.; Wernsdorfer, W.; Christou, G.; Perlepes, S. P. *Polyhedron* **2007**, *26*, 2165. (g) Stamatatos, T. C.; Abboud, K. A.; Wernsdorfer, W.; Christou, G. *Polyhedron* **2007**, *26*, 2042. (h) Stamatatos, T. C.; Abboud, K. A.; Wernsdorfer, W.; Christou, G. *Polyhedron* **2007**, *26*, 2095.

(6) (a) Bagai, R.; Datta, S.; Betancur-Rodriguez, A.; Abboud, K. A.; Hill, S.; Christou, G. *Inorg. Chem.* **2007**, *46*, 4535. (b) Bagai, R.; Abboud, K. A.; Christou, G. *Chem. Commun.* **2007**, 3359. (c) Bagai, R.; Wernsdorfer, W.; Abboud, K. A.; Christou, G. *J. Am. Chem. Soc.* **2007**, *129*, 12918.

(7) (a) Hundal, G.; Hundal, M. S.; Obrai, S.; Poonia, N. S.; Kumar, S. *Inorg. Chem.* **2002**, *41*, 2077. (b) Plass, W. *Eur. J. Inorg. Chem.* **1998**, 799. (c) de Sousa, A. S.; Fernandes, M. A. *Polyhedron* **2002**, *21*, 1883.

(8) Vincent, J. B.; Chang, H. R.; Folting, K.; Huffman, J. C.; Christou, G.; Hendrickson, D. N. *J. Am. Chem. Soc.* **1987**, *109*, 5703.

reflections. A full sphere of data (1850 frames) was collected using the ω-scan method (0.3° frame width). The first 50 frames were remeasured at the end of data collection to monitor instrument and crystal stability (maximum correction on I was <1 %). Absorption corrections by integration were applied based on measured indexed crystal faces. The structure was solved by direct methods in *SHELXTL6* and refined on F^2 using full-matrix least squares. The non-H atoms were treated anisotropically, whereas the hydrogen atoms were placed in ideal, calculated positions and were refined as riding on their respective C atoms.

For **1**·2CH_2Cl_2·MeOH, the asymmetric unit consists of the Mn_8 cation, a benzoate anion, and one MeOH and two CH_2Cl_2 molecules. The solvent molecules were disordered and could not be modeled properly; thus the *SQUEEZE*[9] program, a part of the *PLATON* package of crystallographic software, was used to calculate the solvent disorder area and remove its contribution to the overall intensity data. A total of 1068 parameters were refined in the final cycle of refinement using 10 920 reflections with $I > 2\sigma(I)$ to yield R_1 and R_2 of 3.34 and 8.12%, respectively.

For **2**·6MeCN·$^1/_2H_2O$, the asymmetric unit contains one-quarter of the Mn_{12} cluster, two one-quarter MeCN molecules, one MeCN molecule in a general position, and one-eighth of a water molecule. All solvent molecules were disordered and could not be modeled properly; thus the *SQUEEZE*[9] program was used to calculate the solvent disorder area and remove its contribution to the overall intensity data. A total of 204 parameters were refined in the final cycle of refinement using 2799 reflections with $I > 2\sigma(I)$ to yield R_1 and R_2 of 4.64 and 10.46%, respectively.

For **3**·10MeOH, the asymmetric unit consists of half the Mn_{20} cluster, one ClO_4^- anion, and five MeOH molecules. The latter were disordered and could not be modeled properly; thus the *SQUEEZE*[9] program was again used to calculate the solvent disorder area and remove its contribution to the overall intensity data. The cluster exhibits two disorders: A large part of the N4 ligand is disordered and was refined in two parts; attempts to resolve the two parts of C17′−C18′ were not successful, and thus this part remained common to both. C28 is also disordered and was also refined in two parts. The two parts of each disorder were dependently refined. Three O atoms of the ClO_4^- anion containing Cl2 were also disordered and were refined in two parts related by rotation along the Cl2−O32 axis. A total of 687 parameters were refined in the final cycle of refinement using 6689 reflections with $I > 2\sigma(I)$ to yield R_1 and R_2 of 8.12 and 21.74%, respectively. Unit cell data and details of the structure refinements for the three complexes are listed in Table 1.

Other Studies. Infrared spectra were recorded in the solid state (KBr pellets) on a Nicolet Nexus 670 FTIR spectrometer in the 400−4000 cm^{-1} range. Elemental analyses (C, H, and N) were performed by the in-house facilities of the University of Florida, Chemistry Department. Cl analysis was performed by Complete Analysis Laboratories, Inc., in Parsippany, NJ. Variable-temperature dc and ac magnetic susceptibility data were collected at the University of Florida using a Quantum Design MPMS-XL SQUID susceptometer equipped with a 7 T magnet and operating in the 1.8−300 K range. Samples were embedded in solid eicosane to prevent torquing. Magnetization vs field and temperature data was fit using the program *MAGNET*.[10] Pascal's constants were used to estimate the diamagnetic correction, which was subtracted from the experimental susceptibility to give the molar paramagnetic susceptibility (χ_M).

Table 1. Crystallographic Data for **1**·2CH_2Cl_2·MeOH, **2**·6MeCN·$^1/_2H_2O$, and **3**·10MeOH

	1	**2**	**3**
formula[a]	$C_{80}H_{94}Cl_4Mn_8N_4O_{30}$	$C_{52}H_{99}Cl_8Mn_{12}N_{14}O_{22.5}$	$C_{82}H_{182}Cl_2Mn_{20}N_{12}O_{66}$
fw, g/mol[a]	2172.91	2223.33	3562.05
space group	$P2_1/n$	$P4/ncc$	$P2_1/c$
a, Å	16.0450(16)	19.7797(12)	17.0570(16)
b, Å	17.6428(17)	19.7797(12)	25.409(2)
c, Å	31.896(3)	20.851(2)	15.9322(15)
β, deg	95.425(2)	90	100.463(2)
V, Å^3	8988.6(15)	8157.7(12)	6790.3(11)
Z	4	4	2
T, K	173(2)	173(2)	173(2)
radiation, Å[b]	0.71073	0.71073	0.71073
ρ_{calc}, g/cm^3	1.577	1.810	1.573
μ, mm^{-1}	1.340	2.125	1.886
R_1[c,d]	0.0334	0.0464	0.0812
R_2[e]	0.0812	0.1046	0.2174

[a] Including solvate molecules. [b] Graphite monochromator. [c] $I > 2\sigma(I)$. [d] $R_1 = \sum(||F_o| - |F_c||)/\sum|F_o|$. [e] $R_2 = [\sum[w(F_o^2 - F_c^2)^2]/\sum[w(F_o^2)^2]]^{1/2}$, $w = 1/[\sigma^2(F_o^2) + [(ap)^2 + bp]]$, where $p = [\max(F_o^2, 0) + 2F_c^2]/3$.

Results and Discussion

Syntheses. In order to make clusters containing Mn^{III} ions, it is generally necessary to either oxidize simple Mn^{II} salts or use preformed higher oxidation state Mn_x clusters. Both of these strategies have previously proved to be useful routes to a variety of higher-nuclearity complexes with chelating ligands ranging from bidentate to pentadentate.[4,5,11] Therefore, we decided to employ them both with the potentially hexadentate ligand edteH_4. Thus, a variety of reaction ratios, reagents, and other conditions were investigated. The reaction of edteH_4 with $Mn(O_2CPh)_2$ and NEt_3 in a 1:3:3 molar ratio in MeOH afforded a reddish-brown solution from which was subsequently obtained the octanuclear complex $[Mn_8O_3(OH)(OMe)(O_2CPh)_7(edte)(edteH_2)](O_2CPh)$ (**1**) in ∼20% yield (eq 1). Its formation is summarized in eq 1 where atmospheric oxygen gas is assumed to provide the oxidizing equivalents required to form the mixed-valence

$$8[Mn(O_2CPh)_2] + 2edteH_4 + MeOH + H_2O + {}^3/_2O_2 \rightarrow 8PhCO_2H + [Mn_8O_3(OH)(OMe)(O_2CPh)_7(edte)(edteH_2)](O_2CPh) \quad (1)$$

$6Mn^{III}$, $2Mn^{II}$ product. Complex **1** was also obtained, and in a higher yield of ∼40%, from the reaction of edteH_4 with $[Mn_3O(O_2CPh)_6(py)_2H_2O]$ in a 1:1 molar ratio in CH_2Cl_2/MeOH. Such trinuclear $[Mn_3O(O_2CR)_6(L)_3]^{0,+}$ clusters have often proved to be very useful starting materials for the synthesis of higher-nuclearity products, some of which have

(9) Vandersluis, P.; Spek, A. L. *Acta Crystallogr., Sect. A* **1990**, *46*, 194.
(10) Davidson, E. R. *MAGNET*; Indiana University: Bloomington, IN, 1999.
(11) Tasiopoulos, A. J.; Vinslava, A.; Wernsdorfer, W.; Abboud, K. A.; Christou, G. *Angew. Chem., Int. Ed.* **2004**, *43*, 2117.

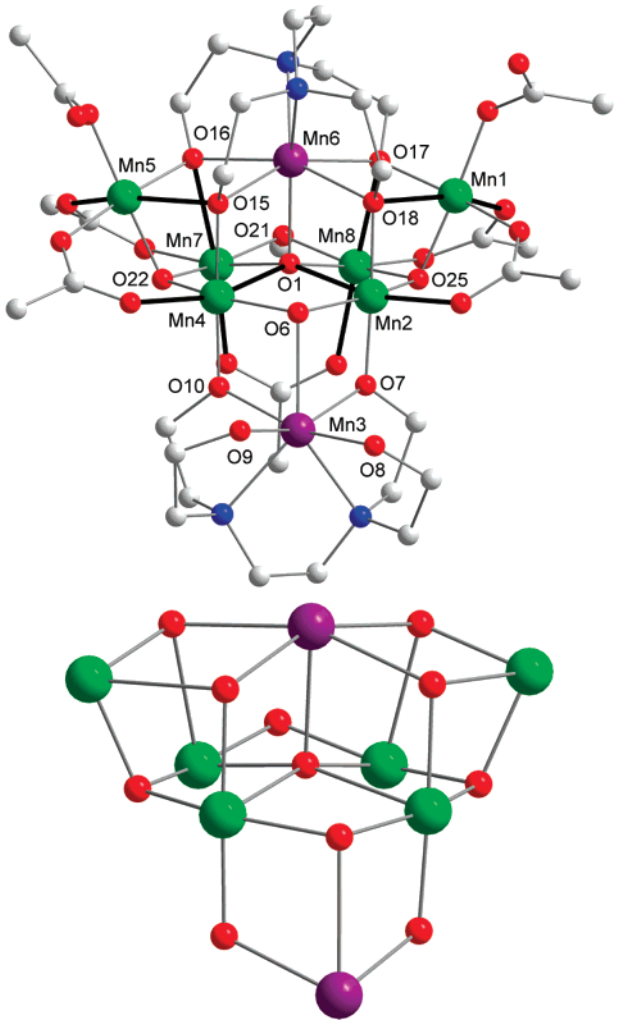

Figure 1. (top) Labeled representation of the cation of **1**. Hydrogen atoms and phenyl rings (except for the ipso carbon atoms) have been omitted for clarity. JT axes are shown as thicker black bonds. (bottom) The core of **1**. Color code: Mn^{III}, green; Mn^{II}, purple; O, red; N, blue; C, gray.

also been new SMMs.[12] The formation of **1** via this route is summarized in eq 2. The mixed solvent system was needed to ensure adequate solubility of all reagents, and it also led

$$3[Mn_3O(O_2CPh)_6(py)_2(H_2O)] + 2edteH_4 + MeOH \rightarrow Mn^{2+} + 6py + 8H^+ + 2H_2O + 10PhCO_2^- + [Mn_8O_3(OH)(OMe)(O_2CPh)_7(edte)(edteH_2)](O_2CPh) \quad (2)$$

to methoxide incorporation; no isolable products were obained when only CH_2Cl_2 was used. Small variations in the Mn/edteH$_4$/PhCO$_2^-$ ratio also gave complex **1**, which clearly is a preferred product of these components and with benzoate. When $[Mn_3O(O_2CR)_6(L)_3]^{0,+}$ clusters with other R groups were employed, we were unable to isolate pure, crystalline materials for satisfactory characterization.

(12) (a) Brechin, E. K.; Boskovic, C.; Wernsdorfer, W.; Yoo, J.; Yamaguchi, A.; Sanudo, E. C.; Concolino, T. R.; Rheingold, A. L.; Ishimoto, H.; Hendrickson, D. N.; Christou, G. *J. Am. Chem. Soc.* **2002**, *124*, 9710. (b) Bagai, R.; Abboud, K. A.; Christou, G. *Dalton Trans.* **2006**, 3306. (c) Maheswaran, S.; Chastanet, G.; Teat, S. J.; Mallah, T.; Sessoli, R.; Wernsdorfer, W.; Winpenny, R. E. P. *Angew. Chem., Int. Ed.* **2005**, *44*, 5044.

Table 2. Selected Bond Distances (Å) and Angles (deg) for **1**·2CH$_2$Cl$_2$·MeOH

Mn1−O3	1.8836(19)	Mn5−O14	1.8923(18)
Mn1−O25	1.8844(17)	Mn5−O22)	1.8941(17
Mn1−O4	1.9492(18)	Mn5−O16	1.9467(18)
Mn1−O17	1.9591(17)	Mn5−O12	1.9517(19)
Mn1−O27	2.176(2)	Mn5−O19	2.195(2)
Mn1−O18	2.3097(18)	Mn5−O15	2.3662(18)
Mn2−O7	1.8554(18)	Mn6−O1	2.2242(17)
Mn2−O25	1.9105(18)	Mn6−O16	2.2495(18)
Mn2−O18	1.9424(17)	Mn6−O18	2.2606(17)
Mn2−O6	1.9566(17)	Mn6−O15	2.2617(18)
Mn2−O5	2.1596(18)	Mn6−O17	2.2647(18)
Mn2−O1	2.4368(17)	Mn6−N4	2.279(2)
Mn3−O10	2.1431(17)	Mn6−N3	2.285(2)
Mn3−O7	2.1543(18)	Mn7−O22	1.8957(18)
Mn3−O8	2.180(2)	Mn7−O1	1.8997(17)
Mn3−O9	2.239(2)	Mn7−O20	1.9505(19)
Mn3−N2	2.330(2)	Mn7−O21	1.9565(18)
Mn3−N1	2.359(2)	Mn7−O23	2.1235(19)
Mn3−O6	2.4054(17)	Mn7−O16	2.3692(18)
Mn4−O10	1.8661(17)	Mn8−O25	1.8937(17)
Mn4−O22	1.9136(18)	Mn8−O1	1.9079(17)
Mn4−O15	1.9297(17)	Mn8−O21	1.9517(18)
Mn4−O6	1.9652(17)	Mn8−O26	1.9571(19)
Mn4−O11	2.1725(19)	Mn8−O24	2.1360(19)
Mn4−O1	2.4695(18)	Mn8−O17	2.3122(18)
Mn7−O1-Mn8	97.12(8)	Mn2−O7−Mn3	109.95(9)
Mn8−O1−Mn2	88.95(6)	Mn4−O10−Mn3	110.16(8)
Mn6−O1−Mn2	92.52(6)	Mn6−O15−Mn5	97.48(7)
Mn7−O1−Mn4	89.31(6)	Mn5−O16−Mn6	111.83(8)
Mn6−O1−Mn4	92.09(6)	Mn8−O21−Mn7	93.83(8)
Mn2−O1−Mn4	80.05(5)	Mn5−O22−Mn7	105.86(8)
Mn2−O6−Mn4	107.14(8)	Mn1−O25−Mn8	104.91(8)
Mn2−O6−Mn3	97.31(7)	Mn4−O6−Mn3	97.19(7)

The reaction of edteH$_4$ with MnCl$_2$·4H$_2$O and NEt$_3$ in 1:2:1 molar ratio in MeCN/MeOH gave a brown solution from which was isolated $[Mn_{12}O_4(OH)_2(edte)_4Cl_6(H_2O)_2]$ (**2**) in 25% yield. As found for **1**, complex **2** is mixed-valent, containing eight Mn^{III} and four Mn^{II} ions, and its formation is summarized in eq 3, again assuming the participation of atmospheric O$_2$. Increasing or decreasing the amount of

$$12MnCl_2 + 4edteH_4 + 4H_2O + 2O_2 \rightarrow [Mn_{12}O_4(OH)_2(edte)_4Cl_6(H_2O)_2] + 18HCl \quad (3)$$

edteH$_4$ or NEt$_3$ also gave complex **2**, but the product was not as pure. We were also unable to isolate any clean products when we employed an MeCN/EtOH solvent system.

Finally, the reaction of edteH$_4$ with Mn(O$_2$CMe)$_2$ and NEt$_3$ in a 1:2:2 ratio in MeOH, followed by the addition of NaClO$_4$, gave a dark orange-brown solution from which was subsequently isolated $[Mn_{20}O_8(OH)_4(O_2CMe)_6(edte)_6](ClO_4)_2$ (**3**) in 20% yield. This product is once again mixed-valent, containing 12 Mn^{III} and 8 Mn^{II} ions, and its formation is summarized in eq 4, with O$_2$ again included as the oxidizing agent.

$$20Mn(O_2CMe)_2 + 6edteH_4 + 6H_2O + 3O_2 \rightarrow [Mn_{20}O_8(OH)_4(O_2CMe)_6(edte)_6]^{2+} + 32MeCO_2H + 2MeCO_2^- \quad (4)$$

It is clear that the described reactions to complexes **1**−**3** are very complicated and involve acid/base and redox chemistry, as well as structural fragmentations and rearrangements. As a result, the reaction solutions likely contain

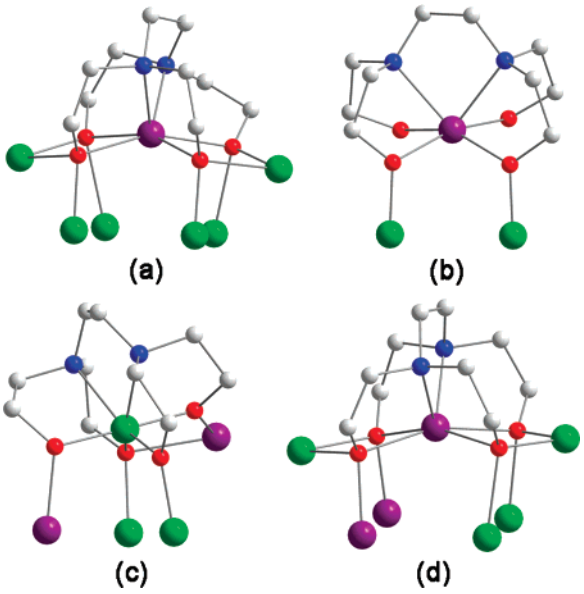

Figure 2. Coordination modes of $edte^{4-}$ and $edteH_2^{2-}$ found in complexes **1**−**3**. Color code: Mn^{III}, green; Mn^{II}, purple; O, red; N, blue; C, gray.

a complicated mixture of several species in equilibrium. For this reason, we were happy to settle for the relatively low yields of **1**−**3**, given that the products were reproducibly obtained in a pure, crystalline form from the described procedures.

Description of Structures. A labeled representation of the $[Mn_8O_3(OH)(OMe)(O_2CPh)_7(edte)(edteH_2)]^+$ cation of **1** is shown in Figure 1, and selected interatomic distances and angles are summarized in Table 2. Complex **1** crystallizes in the monoclinic space group $P2_1/n$. The core is mixed-valence (six Mn^{III}, two Mn^{II}), with Mn3 and Mn6 being the Mn^{II} ions, and contains a $[Mn_7O_7]$ subunit consisting of two distorted $[Mn^{III}_3Mn^{II}(\mu_5\text{-}O)(\mu_3\text{-}O)(\mu_3\text{-}OR)_2]^{5+}$ cubanes sharing the Mn6−O1 edge. This double-cubane unit is additionally bridged by a μ-OMe^- group (O21) between Mn7/Mn8 and a μ_3-OH^- group (O6) between Mn2/Mn4. The latter μ_3-OH^- additionally connects the double cubane to the eighth Mn atom, Mn3. The $edteH_2^{2-}$ group is hexadentate-chelating on Mn^{II} atom Mn3, with the two deprotonated alkoxide O atoms, O7 and O10, bridging to Mn2 and Mn4, respectively, and thus the $edteH_2^{2-}$ group is overall μ_3-bridging; oxygen atoms O8 and O9 are protonated. The $edte^{4-}$ group is also hexadentate-chelating to a Mn^{II} atom, Mn6, with the four deprotonated alkoxide O atoms all adopting μ_3 bridging modes within the double cubane, and thus the $edte^{4-}$ group is overall μ_7-bridging. The chelating/bridging modes of the μ_7-$edte^{4-}$ and μ_3-$edteH_2^{2-}$ groups are shown in parts a and b of Figure 2, respectively. The remaining ligation is provided by seven benzoate groups, five of which are η^1:η^1:μ-bridging, and the remaining two are η^1-terminal on Mn1 and Mn5.

The oxidation states of the Mn atoms and the protonation levels of the O^{2-}, OH^-, OMe^-, and OR^- groups were determined from a combination of charge balance considerations, inspection of bond lengths, and bond valence sum (BVS) calculations.[13] BVS values for Mn and O atoms are listed in Tables 3 and 4, respectively. All the Mn^{III} atoms are six-coordinate and display a Jahn−Teller (JT) elongation, as expected for high-spin Mn^{III} in octahedral geometry, with the JT axes (shown as thicker black bonds in Figure 1, top) not coparallel. The Mn^{II} atoms, Mn3 and Mn6, are seven-coordinate. The anion of complex **1** is a $PhCO_2^-$ group (not shown in Figure 1), which forms an intimate ion pair with the Mn_8 cation by hydrogen bonding with O6 of the μ_3-OH^- ion (O6···O29 = 2.580 Å) and O8 of an $edteH_2^{2-}$ protonated alcohol arm (O8···O28 = 2.584 Å). This also has the effect of raising the BVS of the μ_3-OH^- ion O6 to 1.43, higher than normally expected for a OH^- group (1.0−1.2). The BVS for O8 (1.21) is much less affected by the hydrogen bonding (compare with 1.17 for O9), no doubt due to the only monodentate binding of O8, which thus retains greater basicity and a stronger O−H bond than the μ_3-OH^- ion.

Table 3. BVSs for the Mn Atoms of Complex **1** and **3**[a]

	1			**3**		
atom	Mn^{II}	Mn^{III}	Mn^{IV}	Mn^{II}	Mn^{III}	Mn^{IV}
Mn1	3.21	*2.93*	3.08	*1.85*	1.70	1.78
Mn2	3.18	*2.91*	3.05	3.12	*2.90*	2.98
Mn3	*2.01*	1.87	1.92	3.21	*2.93*	3.08
Mn4	3.13	*2.87*	3.01	2.99	*2.77*	2.85
Mn5	3.14	*2.87*	3.01	*2.48*	2.26	2.38
Mn6	*1.96*	1.83	1.86	3.17	*2.90*	3.04
Mn7	3.17	*2.90*	3.04	3.22	*2.94*	3.09
Mn8	3.18	*2.91*	3.05	*2.45*	2.24	2.35
Mn9				3.05	*2.79*	2.93
Mn10				*1.88*	1.75	1.79

[a] The italicized value is the one closest to the charge for which it was calculated. The oxidation state of a particular atom can be taken as the whole number nearest to the italicized value.

Table 4. BVSs for the O Atoms of Complex **1**[a]

atom	BVS	assignment	group	atom	BVS	assignment	group
O21	1.99	OR^-	OMe^-	O18	1.96	OR^-	$edte^{4-}$
O6	1.43	OH^-	OH^-	O7	2.02	OR^-	$edte^{4-}$
O15	1.95	OR^-	$edte^{4-}$	O8	1.21	ROH	$edteH_2^{2-}$
O16	1.93	OR^-	$edte^{4-}$	O9	1.17	ROH	$edteH_2^{2-}$
O17	1.94	OR^-	$edte^{4-}$	O10	1.98	OR^-	$edte^{4-}$

[a] The BVS values for O atoms of O^{2-}, OH^-, and H_2O groups are typically 1.8−2.0, 1.0−1.2, and 0.2−0.4, respectively, but can be affected somewhat by hydrogen bonding.

A number of other Mn_8 complexes have previously been reported. These possess a variety of metal topologies such as rodlike, serpentine, rectangular, linked Mn_4 butterfly units, linked tetrahedral, etc.,[14] but none have possessed the core of complex **1**, which is unprecedented. In addition to this novel core structure, another unusual feature of **1** is the presence of its μ_5-O^{2-} ion, O1. There are only two previous structural types with a μ_5-O^{2-} ion in molecular Mn chemistry, certain Mn_{12}[15] and Mn_{13}[16] complexes.

The labeled structure of **2** is shown in Figure 3, and selected interatomic distances and angles are listed in Table 5. Complex **2** crystallizes in the tetragonal space group $P4/ncc$ with the Mn_{12} molecule lying on an S_4 symmetry axis

(13) (a) Liu, W. T.; Thorp, H. H. *Inorg. Chem.* **1993**, *32*, 4102. (b) Palenik, G. J. *Inorg. Chem.* **1997**, *36*, 4888. (c) Brown, I. D.; Wu, K. K. *Acta Crystallogr., Sect. B: Struct. Sci.* **1976**, *32*, 1957.

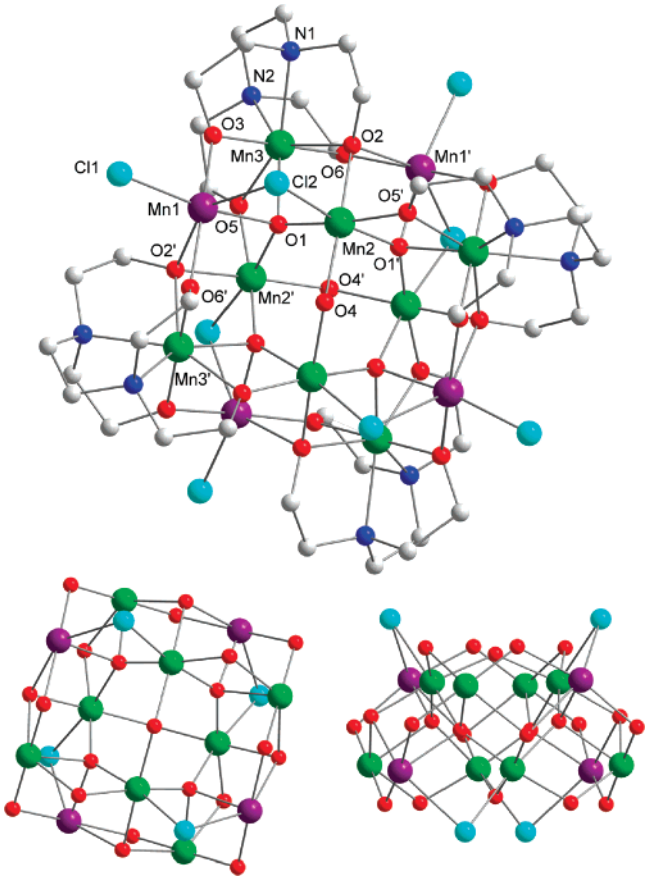

Figure 3. (top) Labeled representation of the structure of **2**. (bottom) The core of **2** viewed along (left) the *c* axis and (right) the *b* axis. Color code: Mn^{III}, green; Mn^{II}, purple; Cl, cyan; O, red; N, blue; C, gray.

and thus only one-quarter of it in the asymmetric unit. The structure consists of a $[Mn^{III}_8Mn^{II}_4(\mu_4\text{-}O)_4(\mu\text{-}OH)_2(\mu\text{-}Cl)_4(\mu_3\text{-}OR)_4(\mu\text{-}OR)_{12}]^{2+}$ core consisting of two near-planar Mn_6 layers sandwiched between three near-planar layers of O atoms (Figure 3, bottom). For the sake of brevity, reference to specific atoms in the following discussion includes their symmetry-related partners. BVS calculations for the Mn atoms (Table 6) identified Mn1, Mn2, and Mn3 as Mn^{II}, Mn^{III}, and Mn^{III} atoms, respectively. Mn1 and Mn2 are six-coordinate while Mn3 is seven-coordinate. The 4 μ_4-O^{2-} ions (O1) together serve to connect all 12 Mn atoms. Each $edte^{4-}$ group is hexadentate-chelating on a Mn^{III} atom, Mn3, with each of its deprotonated alkoxide arms bridging to either one (O3, O5, O6) or two (O2) additional Mn atoms. Thus, the $edte^{4-}$ groups are overall μ_5-bridging, as shown in Figure 2c.

Charge balance considerations require that, with eight Mn^{III}, four Mn^{II}, four O^{2-}, and four $edte^{4-}$ groups, there must be eight additional negatively charged ligands to give neutral complex **2**. The simplest conclusion is that with eight apparent Cl^- ions in the complex, the two μ-O atoms O4 and O4′ bridging Mn2 atoms belong to H_2O groups. However, we were unhappy with this conclusion, being unaware of any precedent in the literature for H_2O groups

Table 5. Selected Bond Distances (Å) and Angles (deg) for **2**·6MeCN·$^1/_2H_2O$

Mn1−O6′	2.065(3)	Mn2−O1′	2.033(3)
Mn1−O3	2.088(3)	Mn2−Cl2	2.5255(14)
Mn1−O1	2.138(3)	Mn3−O6	1.882(3)
Mn1−O2′	2.306(3)	Mn3−O3	1.905(3)
Mn1−Cl1	2.4050(13)	Mn3−O5	2.107(2)
Mn1−Cl2	2.5813(14)	Mn3−O1	2.163(3)
Mn2−O1	1.841(2)	Mn3−O2	2.209(3)
Mn2−O5′	1.910(2)	Mn3−N2	2.275(3)
Mn2−O4	2.0098(15)	Mn3−N1	2.320(3)
Mn2−O2	2.015(3)		
		O2−Mn2−Cl2	92.62(8)
Mn2−O4−Mn2′	133.9(2)	O2−Mn2−Cl2	92.62(8)
O6′−Mn1−O3	168.16(11)	O1′−Mn2−Cl2	171.93(8)
O2′−Mn1−Cl1	108.95(7)	O6−Mn3−O5	87.60(11)
O1−Mn1−Cl2	82.17(7)	O5−Mn3−O1	72.73(9)
O2′−Mn1−Cl2	147.38(7)	O3−Mn3−O2	105.80(11)
O1−Mn2−O5′	172.08(12)	O5−Mn3−N2	75.17(10)
O1−Mn2−O4	92.17(10)	O6−Mn3−N1	100.89(12)

Table 6. BVSs[a] for the Mn and O Atoms of Complex **2**

	manganese BVSs				oxygen BVSs		
atom	Mn^{II}	Mn^{III}	Mn^{IV}	atom	BVS	assignment	group
Mn1	*2.23*	2.12	2.17	O1	1.98	O^{2-}	O^{2-}
Mn2	3.34	*3.09*	3.22	O4	0.99	OH^-	OH^-
Mn3	3.05	*2.82*	2.91	O2	1.89	OR^-	$edte^{4-}$
				O3	1.97	OR^-	$edte^{4-}$
				O5	1.97	OR^-	$edte^{4-}$
				O6	2.03	OR^-	$edte^{4-}$

[a] See the footnotes to Tables 3 and 4.

bridging two Mn^{III} atoms; the high Lewis acidity of two Mn^{III} atoms would be expected to make the water molecule in a $[Mn^{III}_2(\mu\text{-}OH_2)]$ unit very (Brønsted) acidic (very low pK_a) and unlikely to be stable. In contrast, a water molecule

(14) (a) Godbole, M. D.; Roubeau, O.; Clerac, R.; Kooijman, H.; Spek, A. L.; Bouwman, E. *Chem. Commun.* **2005**, 3715. (b) Brechin, E. K.; Soler, M.; Christou, G.; Helliwell, M.; Teat, S. J.; Wernsdorfer, W. *Chem. Commun.* **2003**, 1276. (c) Rajaraman, G.; Murugesu, M.; Sanudo, E. C.; Soler, M.; Wernsdorfer, W.; Helliwell, M.; Muryn, C.; Raftery, J.; Teat, S. J.; Christou, G.; Brechin, E. K. *J. Am. Chem. Soc.* **2004**, *126*, 15445. (d) Murugesu, M.; Wernsdorfer, F.; Abboud, K. A.; Christou, G. *Angew. Chem., Int. Ed.* **2005**, *44*, 892. (e) Brechin, E. K.; Christou, G.; Soler, M.; Helliwell, M.; Teat, S. J. *Dalton Trans.* **2003**, 513. (f) Jones, L. F.; Brechin, E. K.; Collison, D.; Raftery, J.; Teat, S. J. *Inorg. Chem.* **2003**, *42*, 6971. (g) Tsai, H. L.; Wang, S. Y.; Folting, K.; Streib, W. E.; Hendrickson, D. N.; Christou, G. *J. Am. Chem. Soc.* **1995**, *117*, 2503. (h) Tanase, S.; Aromi, G.; Bouwman, E.; Kooijman, H.; Spek, A. L.; Reedijk, J. *Chem. Commun.* **2005**, 3147. (i) Milios, C. J.; Kefalloniti, E.; Raptopoulou, C. P.; Terzis, A.; Vicente, R.; Lalioti, N.; Escuer, A.; Perlepes, S. P. *Chem. Commun.* **2003**, 819. (j) Alvareza, C. S.; Bond, A. D.; Cave, D.; Mosquera, M. E. G.; Harron, E. A.; Layfield, R. A.; McPartlin, M.; Rawson, J. M.; Wood, P. T.; Wright, D. S. *Chem. Commun.* **2002**, 2980. (k) Boskovic, C.; Huffman, J. C.; Christou, G. *Chem. Commun.* **2002**, 2502. (l) Saalfrank, R. W.; Low, N.; Demleitner, B.; Stalke, D.; Teichert, M. *Chem.—Eur. J.* **1998**, *4*, 1305. (m) Wemple, M. W.; Tsai, H. L.; Wang, S. Y.; Claude, J. P.; Streib, W. E.; Huffman, J. C.; Hendrickson, D. N.; Christou, G. *Inorg. Chem.* **1996**, *35*, 6437. (n) Tasiopoulos, A. J.; Abboud, K. A.; Christou, G. *Chem. Commun.* **2003**, 580. (o) Milios, C. J.; Fabbiani, F. P. A.; Parsons, S.; Murugesu, M.; Christou, G.; Brechin, E. K. *Dalton Trans.* **2006**, 351. (p) Saalfrank, R. W.; Low, N.; Trummer, S.; Sheldrick, G. M.; Teichert, M.; Stalke, D. *Eur. J. Inorg. Chem.* **1998**, 559.

(15) (a) Murugesu, M.; Wernsdorfer, W.; Abboud, K. A.; Brechin, E. K.; Christou, G. *Dalton Trans.* **2006**, 2285. (b) Li, Y. G.; Wernsdorfer, W.; Clerac, R.; Hewitt, I. J.; Anson, C. E.; Powell, A. K. *Inorg. Chem.* **2006**, *45*, 2376.

(16) (a) Lampropoulos, C.; Murugesu, M.; Abboud, K. A.; Christou, G. *Polyhedron* **2007**, *26*, 2129. (b) Masello, A.; Murugesu, M.; Abboud, K. A.; Christou, G. *Polyhedron* **2007**, *26*, 2276. (c) Sun, Z. M.; Gantzel, P. K.; Hendrickson, D. N. *Inorg. Chem.* **1996**, *35*, 6640.

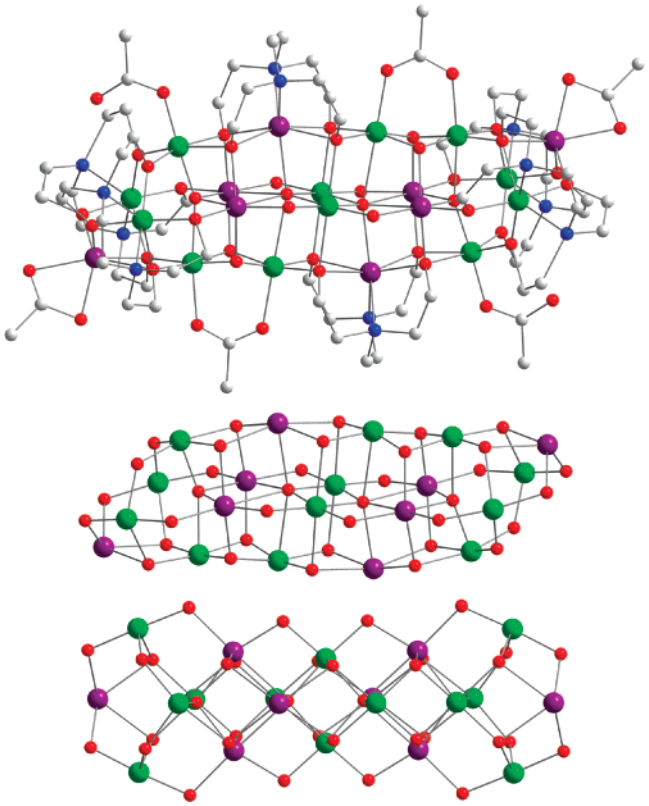

Figure 4. (top) Structure of the cation of **3**. (middle and bottom) The core of **3** from different viewpoints emphasizing the 3 × 2 cubane arrangement. Color code: Mn^{III}, green; Mn^{II}, purple; O, red; N, blue; C, gray.

bridging two Mn^{II} atoms is known.[17] We thus decided to determine the protonation levels of all O atoms in **2** by BVS calculations, and the results are listed in Table 6. The oxide and $edte^{4-}$ O atoms have BVS values of >1.89, confirming them as completely deprotonated, as concluded above from their bridging modes. In contrast, O4 has a BVS of only 0.99, as expected for an OH^- group. In addition, the Mn2−O4 bond length of 2.0098(15) Å is typical of Mn^{III}−OH^- bond lengths in the literature.[18] This is a more realistic bridging group between two Mn^{III} atoms and is also consistent with the steric congestion about O4 as a result of the encroachment near O4 by the $edte^{4-}$ CH_2 groups; a space-filling representation of **2** is provided in the Supporting Information. Thus, we conclude that O4 and O4′ are OH^- groups. This now requires six additional anionic ligands for a neutral molecule, and we suspected that the S_4 symmetry was masking a disorder between the Cl^- ion and a neutral ligand such as H_2O at the terminal positions (Cl1). Crystallographic refinement of these terminal Cl atoms was inconclusive as to whether there was a Cl/H_2O disorder, and so we investigated the Cl content of the molecule more directly with a chlorine elemental analysis. This did indeed give a value less than expected for eight Cl atoms, whose formula of $[Mn_{12}O_4(H_2O)_2(edte)_4Cl_8]$ would have a calculated 14.40% Cl content, much higher than the experimental value of 11.89%. The latter is, however, consistent with the expected six Cl^- ions that are required for the observed neutrality of complex **2** if O4 is a OH^- ion. Thus, we conclude that the correct formula of **2** is $[Mn_{12}O_4(OH)_2(edte)_4Cl_6(H_2O)_2]$. Note that for the reasons already mentioned, we disfavor the H_2O groups being disordered with Cl at the μ-Cl^- positions (Cl2) bridging $Mn^{III}Mn^{II}$ pairs, but this is not as unlikely as water bridging two Mn^{III} atoms, and thus cannot be completely ruled out. Indeed, maybe the two water molecules are disordered among the eight bridging and terminal positions, and this is why the crystallographic refinement is fine with eight Cl atoms. It should also be noted that while this manuscript was in preparation, a complex apparently identical to complex **2** was reported by Zhou et al.,[19] but who instead formulated it as $[Mn_{12}O_4(H_2O)_2(edte)_4Cl_8]$.[20]

There are many other structural types of Mn_{12} complexes already in the literature, the most well-studied being the $[Mn_{12}O_{12}(O_2CR)_{16}(H_2O)_4]$ (Mn_{12}) family, which has been extended over the years to include one-, two-, and three-electron reduced $[Mn_{12}]^{z-}$ ($z = 0-3$) versions.[21] Another Mn_{12} family of complexes was more recently obtained by reductive aggregation of MnO_4^- in MeOH-containing media; this family differs from the previous one in having a central Mn^{IV}_4 rhombus rather than a Mn^{IV}_4 tetrahedron.[22] The remaining Mn_{12} complexes cover a variety of other structural

(17) (a) Caneschi, A.; Ferraro, F.; Gatteschi, D.; Melandri, M. C.; Rey, P.; Sessoli, R. *Angew. Chem., Int. Ed.* **1989**, *28*, 1365. (b) Yu, S. B.; Lippard, S. J.; Shweky, I.; Bino, A. *Inorg. Chem.* **1992**, *31*, 3502. (c) Ye, B. H.; Mak, T; Williams, I. D.; Li, X. Y. *Chem. Commun.* **1997**, 1813. (d) Coucouvanis, D.; Reynolds, R. A., III; Dunham, W. R. *J. Am. Chem. Soc.* **1995**, *117*, 7570.

(18) (a) Cheng, B. S.; Fries, P. H.; Marchon, J. C.; Scheidt, W. R. *Inorg. Chem.* **1996**, *35*, 1024. (b) Komatsuzaki, H.; Ichikawa, S.; Hikichi, S.; Akita, M.; Moro-oka, Y. *Inorg. Chem.* **1998**, *37*, 3652. (c) Biswas, S.; Mitra, K.; Adhikary, B.; Lucas, C. R. *Transition Met. Chem.* **2005**, *30*, 586.

(19) Zhou, A. J.; Qin, L. J.; Beedle, C. C.; Ding, S.; Nakano, M.; Leng, J. D.; Tong, M. L.; Hendrickson, D. N. *Inorg. Chem.* **2007**, *46*, 8111.

(20) The compound was prepared from a reaction mixture containing both Mn and Fe, and there are no elemental analysis data provided, so it is difficult for us to comment further on the exact formulation. We note, however, that the ostensibly Mn^{II} sites gave a very high BVS of 2.68, and the bridging water O atoms have a BVS of ~1.0, as in our complex **2**. The magnetic data for this compound are also very different from those for our complex **2**; specifically, they indicate a smaller ground-state spin of $S \sim 3$, consistent with stronger antiferromagnetic interactions, as would be expected if the compound contained some Fe^{III}.

(21) (a) Lis, T. *Acta Crystallogr., Sect. B: Struct. Sci.* **1980**, *36*, 2042. (b) Eppley, H. J.; Tsai, H. L.; Devries, N.; Folting, K.; Christou, G.; Hendrickson, D. N. *J. Am. Chem. Soc.* **1995**, *117*, 301. (c) Soler, M.; Wernsdorfer, W.; Abboud, K. A.; Huffman, J. C.; Davidson, E. R.; Hendrickson, D. N.; Christou, G. *J. Am. Chem. Soc.* **2003**, *125*, 3576. (d) Chakov, N. E.; Soler, M.; Wernsdorfer, W.; Abboud, K. A.; Christou, G. *Inorg. Chem.* **2005**, *44*, 5304. (e) Bian, G. Q.; Kuroda-Sowa, T.; Konaka, H.; Hatano, M.; Maekawa, M.; Munakata, M.; Miyasaka, H.; Yamashita, M. *Inorg. Chem.* **2004**, *43*, 4790. (f) Zhao, H. H.; Berlinguette, C. P.; Bacsa, J.; Prosvirin, A. V.; Bera, J. K.; Tichy, S. E.; Schelter, E. J.; Dunbar, K. R. *Inorg. Chem.* **2004**, *43*, 1359. (g) Coronado, E.; Torment-Aliaga, A.; Gaita-Arino, A.; Giminez-Saiz, C.; Romero, F. M.; Wernsdorfer, W. *Angew. Chem., Int. Ed.* **2004**, *43*, 6152. (h) Soler, M.; Wernsdorfer, W.; Abboud, K. A.; Hendrickson, D. N.; Christou, G. *Polyhedron*, **2003**, *22*, 1777. (i) Bagai, R.; Christou, G. *Inorg. Chem.* **2007**, *46*, 10810.

(22) (a) Tasiopoulos, A. J.; Wernsdorfer, W.; Abboud, K. A.; Christou, G. *Inorg. Chem.* **2005**, *44*, 6324. (b) King, P.; Wernsdorfer, W.; Abboud, K. A.; Christou, G. *Inorg. Chem.* **2005**, *44*, 8659.

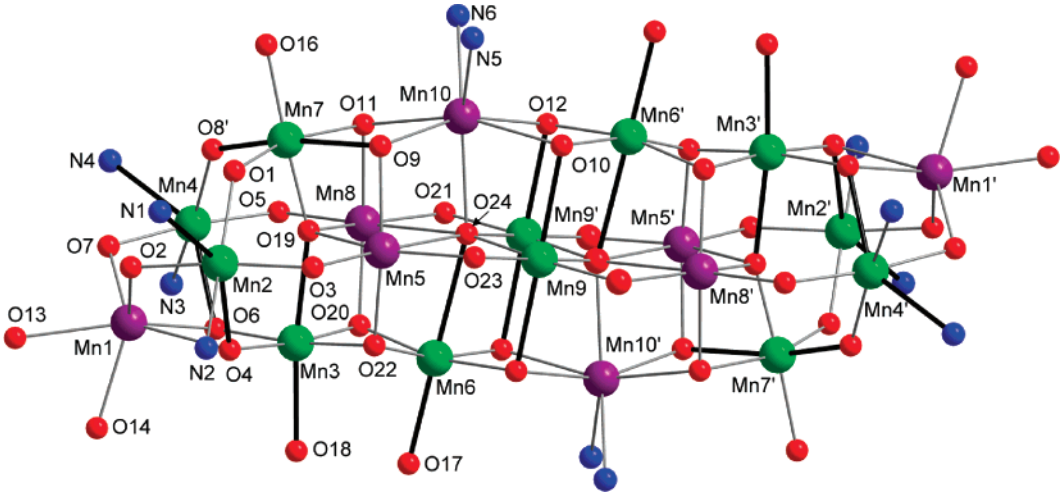

Figure 5. Labeled representation of the core of **3**. JT axes are shown as thicker black bonds. Color code: Mn^{III}, green; Mn^{II}, purple; O, red; N, blue.

types, including loops and more complicated face-sharing cuboidal units, among others.[14c,15,23]

The structure of the cation of **3** is shown in Figures 4 and 5, the latter providing the atom labeling. Selected interatomic distances and angles are listed in Table 7. Complex **3** crystallizes in the monoclinic space group $P2_1/c$ with the Mn_{20} cation lying on a crystallographic inversion center; again, reference to a specific atom will include its symmetry-related partner. The cation can be described as consisting of two sets of three edge-sharing $[Mn_4O_4]$ cubanes (Figure 4, middle), with the upper and lower sets connected by face-sharing to give a 3×2 arrangement of six cubanes. This central $[Mn_{14}O_{16}]$ unit is then attached to three additional Mn ions at each end by additional O atoms (Figure 4, bottom). This gives an overall tubelike arrangement of 20 Mn atoms inside of which are 4 O^{2-} ions. Note that the Mn_7 edge-sharing double-cubane structure of complex **1** is a recognizable subfragment of the central $[Mn_{14}O_{16}]$ unit of **3**, and thus **3** can be considered a more extended version of **1**. The overall core is thus $[Mn^{III}_{12}Mn^{II}_8(\mu_6\text{-}O)_2(\mu_4\text{-}O)_2(\mu_3\text{-}O)_4(\mu\text{-}OH)_4(\mu_3\text{-}OR)_{10}(\mu\text{-}OR)_{14}]^{2+}$ with the two μ_6-O (O24), two μ_4-O (O19), and four μ_3-O (O20, O22) atoms being O^{2-} ions. The four μ-OH^- groups (O21 and O23)[24] bridge Mn8/Mn9′ and Mn5/Mn9, respectively, and thus provide additional linkages between the cubanes. The 10 μ_3-OR and 14 μ-OR oxygen atoms are provided by the alkoxide arms of 6 $edte^{4-}$ groups. As seen in **1** and **2**, each $edte^{4-}$ group binds as a hexadentate chelate to one Mn and then bridges through its deprotonated alkoxide arms to a number of additional Mn atoms; four $edte^{4-}$ groups are overall μ_5-bridging, the remaining two are μ_7-bridging, and these modes are shown in parts c and d of Figure 2, respectively. The remaining ligation in the molecule is provided by six acetate groups, two of which are η^1:η^1:μ-bridging, two are η^2-chelating on Mn1, and two are η^1-terminal on Mn7.

Inspection of metric parameters and BVS calculations (Table 3) indicates that there are 12 Mn^{III} and 8 Mn^{II} atoms

Table 7. Selected Bond Distances (Å) and Angles (deg) for **3**·10MeOH

Mn1−O2	2.111(7)	Mn6−O22	1.890(6)
Mn1−O7	2.116(7)	Mn6−O20	1.900(5)
Mn1−O14	2.148(11)	Mn6−O10′	1.927(6)
Mn1−O13	2.258(9)	Mn6−O12′	1.944(5)
Mn1−O6	2.293(7)	Mn6−O17	2.132(6)
Mn1−O4	2.333(6)	Mn6−O24	2.523(5)
Mn2−O2	1.874(6)	Mn7−O19	1.856(6)
Mn2−O3	1.903(5)	Mn7−O16	1.919(6)
Mn2−O1	1.926(7)	Mn7−O1	1.979(7)
Mn2−N2	2.165(7)	Mn7−O8′	2.002(8)
Mn2−O4	2.175(6)	Mn7−O11	2.142(8)
Mn2−N1	2.308(8)	Mn7−O9	2.177(7)
Mn3−O20	1.882(6)	Mn8−O21	1.990(6)
Mn3−O22	1.895(6)	Mn8−O20	1.999(6)
Mn3−O6	1.973(6)	Mn8−O11	2.039(7)
Mn3−O4	1.988(6)	Mn8−O5	2.121(6)
Mn3−O18	2.130(6)	Mn8−O19	2.128(8)
Mn3−O19	2.227(6)	Mn8−O24	2.498(5)
Mn4−O5	1.892(7)	Mn9−O23	1.916(6)
Mn4−O7	1.910(7)	Mn9−O21′	1.929(6)
Mn4−O8′	1.934(8)	Mn9−O24′	1.939(5)
Mn4−N3	2.159(9)	Mn9−O24	1.946(5)
Mn4−O6	2.228(6)	Mn9−O10	2.270(5)
Mn4−N4′	2.35(2)	Mn9−O12′	2.270(5)
Mn4−N4	2.356(16)	Mn10−O9	2.229(6)
Mn5−O22	1.986(6)	Mn10−O12	2.246(6)
Mn5−O23	1.994(5)	Mn10−O11	2.260(6)
Mn5−O9	2.040(6)	Mn10−O10	2.264(6)
Mn5−O19	2.085(7)	Mn10−N6	2.303(8)
Mn5−O3	2.145(6)	Mn10−N5	2.304(8)
Mn5−O24	2.502(5)	Mn10−O24	2.334(5)
Mn2−O1−Mn7	128.2(4)	Mn10−O10−Mn9	93.0(2)
Mn2−O2−Mn1	110.8(3)	Mn8−O11−Mn7	95.2(3)
Mn2−O3−Mn5	110.8(3)	Mn6′−O12−Mn9′	99.1(2)
Mn3−O4−Mn2	118.9(3)	Mn7−O19−Mn8	101.4(3)
Mn4−O5−Mn8	113.5(3)	Mn3−O20−Mn6	93.3(3)
Mn4−O6−Mn1	92.3(2)	Mn9′−O21−Mn8	106.8(3)
Mn4−O7−Mn1	108.0(3)	Mn3−O22−Mn5	104.3(2)
Mn4−O8′−Mn7	130.6(4)	Mn9−O23−Mn5	106.6(3)
Mn7−O9−Mn10	104.3(3)	Mn9−O24−Mn10	100.0(2)

(23) (a) Foguet-Albiol, D.; O'Brien, T. A.; Wernsdorfer, W.; Moulton, B.; Zaworotko, M. J.; Abboud, K. A.; Christou, G. *Angew. Chem., Int. Ed.* **2005**, *44*, 897. (b) Boskovic, C.; Brechin, E. K.; Streib, W. E.; Folting, K.; Hendrickson, D. N.; Christou, G. *Chem. Commun.* **2001**, 467. (c) Murugesu, M.; Wernsdorfer, W.; Abboud, K. A.; Brechin, E. K.; Christou, G. *Dalton Trans.* **2006**, 2285. (d) Boskovic, C.; Brechin, E. K.; Streib, W. E.; Folting, K.; Bollinger, J. C.; Hendrickson, D. N.; Christou, G. *J. Am. Chem. Soc.* **2002**, *124*, 3725. (e) Rumberger, E. M.; Shah, S. J.; Beedle, C. C.; Zakharov, L. N.; Rheingold, A. L.; Hendrickson, D. N. *Inorg. Chem.* **2005**, *44*, 2742. (f) Yao, H. C.; Li, Y. Z.; Song, Y.; Ma, Y. S.; Zheng, L. M.; Xin, X. Q. *Inorg. Chem.* **2006**, *45*, 59. (g) Dendrinou-Samara, C.; Zaleski, C. M.; Evagorou, A.; Kampf, J. W.; Pecoraro, V. L.; Kessissoglou, D. P. *Chem. Commun.* **2003**, 2668.

(24) The BVS values for O21 and O23 are 1.19 and 1.20, respectively.

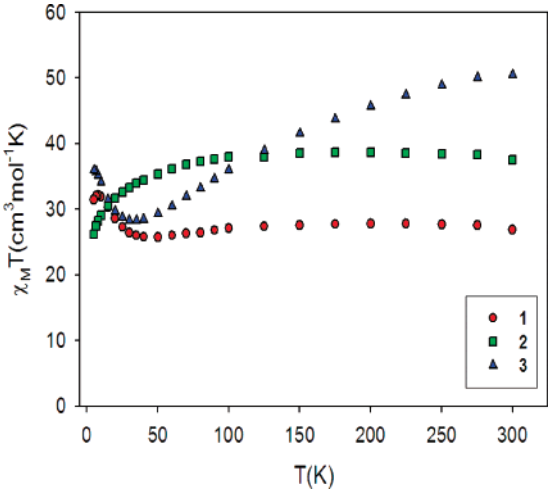

Figure 6. Plots of $\chi_M T$ vs T for complexes **1**·2H$_2$O (●), **2** (■), and **3**·5H$_2$O (▲).

in the molecule. The BVS values for Mn5 and Mn8 are a little higher than normally expected for Mn^{II}, and those for Mn4 and Mn9 are a little lower than normally expected for Mn^{III}, so it is possible that there is some Mn^{II}/Mn^{III} static disorder within the core. All the Mn ions are six-coordinate except Mn5, which is seven-coordinate. The JT elongation axes on six-coordinate Mn^{III} atoms are shown as thicker black bonds in Figure 5. There is only one other Mn_{20} cluster in the literature, a complex with benzylphosphonate ligands reported by Winpenny and co-workers,[12c] which contains 12 Mn atoms in 1 plane. Complex **3** is thus structurally very different from this previous example. In addition to the novel overall structure, there is again, as for **1**, another unusual feature, namely, the presence of μ_6-O^{2-} ions (O24). There are only two previous examples of such a μ_6-O^{2-} ion in Mn chemistry, $[Mn_{10}O_2Cl_8(thme)_6]^{2-}$ and $[Mn_{18}O_{14}(OMe)_{14}(O_2CBu^t)_8(MeOH)_6]$.[25]

Magnetochemistry. Solid-state, variable-temperature dc magnetic susceptibility data in a 0.1 T field and in the 5.0−300 K range were collected on powdered microcrystalline samples of **1**·2H$_2$O, **2**, and **3**·5H$_2$O restrained in eicosane. The obtained data are plotted as $\chi_M T$ vs T in Figure 6. The $\chi_M T$ values at 300 K are 26.8, 37.5, and 50.4 cm^3 K mol^{-1} for **1**−**3**, respectively. The 300 K value is equal to or less than the spin-only ($g = 2$) value of 26.75, 41.5, and 71.0 cm^3 K mol^{-1} expected for noninteracting Mn$^{III}_6$Mn$^{II}_2$, Mn$^{III}_8$Mn$^{II}_4$, and Mn$^{III}_{12}$Mn$^{II}_8$ mixed-valence situations of **1**−**3**, respectively. For **1**·2H$_2$O, $\chi_M T$ stays essentially constant with decreasing temperature until 25 K and then increases to 32.1 cm^3 K mol^{-1} at 8.0 K before dropping slightly to 31.4 cm^3 K mol^{-1} at 5.0 K. The $\chi_M T$ value at the lowest temperatures suggests an $S = 8$ ground-state spin with $g < 2$, as expected for Mn. For **2**, $\chi_M T$ again stays essentially constant with decreasing temperature until 70 K and then decreases smoothly to 26.2 cm^3 K mol^{-1} at 5.0 K, which is suggestive of an $S = 7$ ground state. For **3**·5H$_2$O, $\chi_M T$ decreases smoothly with decreasing temperature to a minimum of 28.2 cm^3 mol^{-1} K at 35 K and then increases to 36.0 cm^3 K mol^{-1} at 5.0 K, which again suggests an $S = 8$ ground state.

To confirm the above initial estimates of the ground-state spin of the three compounds, variable-field (H) and variable-temperature magnetization (M) data were collected in the 0.1−7 T and 1.8−10 K ranges. The resulting data for **1**·2H$_2$O are plotted in Figure 7 as reduced magnetization ($M/N\mu_B$) vs H/T, where N is Avogadro's number and μ_B is the Bohr magneton. The data were fit, using the program *MAGNET*,[10] by diagonalization of the spin Hamiltonian matrix assuming only the ground state is populated, incorporating axial anisotropy ($D\hat{S}_z^2$) and Zeeman terms, and employing a full powder average. The corresponding spin Hamiltonian is given by eq 5, where

$$\mathscr{H} = D\hat{S}_z^{\,2} + g\mu_B\mu_0\hat{S}\cdot H \qquad (5)$$

$\hat{S}_z$ is the easy-axis spin operator, g is the Landé g factor, and μ_0 is the vacuum permeability. The last term in eq 5 is the Zeeman energy associated with the applied magnetic field. The best fit for **1**·2H$_2$O is shown as the solid lines in Figure 7 (top) and was obtained with $S = 8$, $g = 2.00$, and $D = -0.30$ cm^{-1}. Alternative fits with $S = 7$ and $S = 9$ gave unreasonable values of g of 2.28 and 1.78, respectively. In order to ensure that the true global minimum had been located and to assess the hardness of the fit, a root-mean-square (rms) D vs g error surface for the fit was generated using the program *GRID*,[26] which calculates the relative difference between the experimental $M/N\mu_B$ data and those calculated for various combinations of D and g. This is shown as a two-dimensional contour plot in Figure 8 covering the $D = -0.10$ to -0.50 cm^{-1} and $g = 1.90-2.10$ ranges. Only one minimum was observed, and this was a relatively soft minimum; we thus estimate the fit uncertainties as $D = -0.30 \pm 0.01$ cm^{-1} and $g = 2.00 \pm 0.02$.

For **2**, we could not obtain a satisfactory fit if data collected at all field values were employed. In our experience, the usual reason for this is the presence of low-lying excited states because (i) the excited states are close enough to the ground state and they have a nonzero Boltzmann population even at the low temperatures used in the magnetization data collection and/or (ii) even excited states that are more separated from the ground state but that have an S value greater than that of the ground state become populated as their larger M_S levels rapidly decrease in energy in the applied dc magnetic field and approach (or even cross) those of the ground state. Either (or both) of these two effects will lead to poor fits because the fitting program assumes population of only the ground state. A large density of low-lying excited states is expected for higher-nuclearity complexes and/or those with a significant content of Mn^{II} atoms, which give weak exchange couplings. Thus, it is reasonable that such problems are more likely for **2** than for **1**, given both the higher nuclearity and the higher relative Mn^{II} content

(25) (a) Cavaluzzo, M.; Chen, Q.; Zubieta, J. *Chem. Commun.* **1993**, 131. (b) Koo, B. K.; Lee, U. *Bull. Korean Chem. Soc.* **2001**, *22*, 103. (c) Brechin, E. K.; Clegg, W.; Murrie, M.; Parsons, S.; Teat, S. J.; Winpenny, R. E. P. *J. Am. Chem. Soc.* **1998**, *120*, 7365.

(26) Davidson, E. R. *GRID*; Indiana University: Bloomington, IN, 1999.

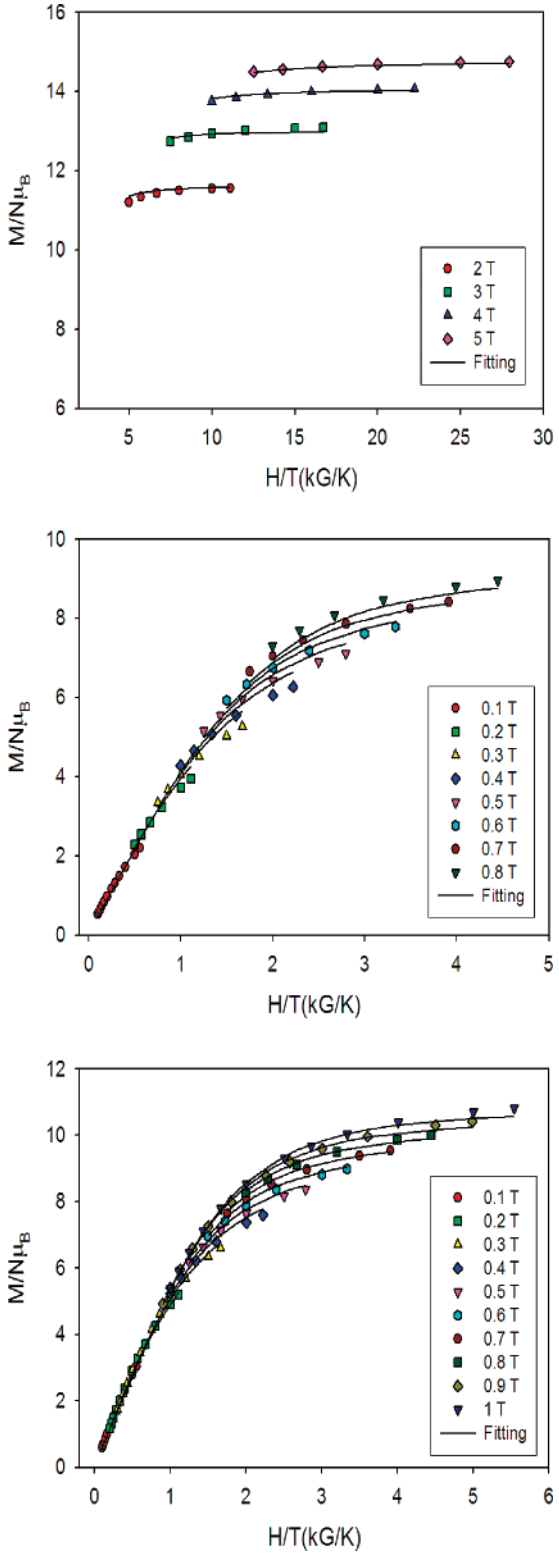

Figure 7. Plots of reduced magnetization ($M/N\mu_B$) vs H/T for complexes **1**·2H$_2$O (top), **2** (middle), and **3**·5H$_2$O (bottom). The solid lines are the fits of the data; see the text for the fit parameters.

of **2** vs **1**. As we have described elsewhere,[22,27,28] one way around effect ii is to use only data collected at low fields. Indeed, a satisfactory fit (solid lines in Figure 7, middle) was now obtained using data in fields up to 0.8 T, with fit parameters $S = 7$, $D = -0.16$ cm^{-1}, and $g = 1.90$.[20]

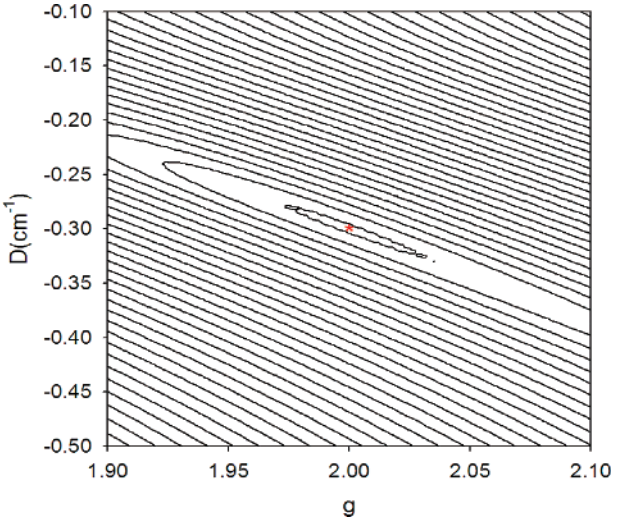

Figure 8. Two-dimensional contour plot of the rms error surface vs D and g for the magnetization fit for **1**·2H$_2$O.

Alternative fits with $S = 6$ and $S = 8$ gave $g = 2.20$ and 1.67, respectively. The corresponding error surface vs D and g (see Supporting Information) gives a harder minimum than that for **1**, with estimated fit uncertainties of $D = -0.16 \pm 0.01$ cm^{-1} and $g = 1.90 \pm 0.01$.

For **3**·5H$_2$O, the even higher metal nuclearity and Mn^{II} content again necessitated using data collected at lower fields in the fit, and in this case a satisfactory fit (solid lines in Figure 7, bottom) was obtained for data up to 1 T with fit parameters $S = 8$, $g = 1.90$, and $D = -0.16$ cm^{-1}. Alternative fits with $S = 7$ and $S = 9$ gave $g = 2.16$ and 1.70, respectively. The corresponding error surface vs D and g (see Supporting Information) is similar to that for **2** and gives estimated fit uncertainties of $D = -0.16 \pm 0.01$ cm^{-1} and $g = 1.90 \pm 0.01$.

The magnetization fits confirmed the preliminary estimates of the ground-state spin S values of **1**−**3**, but we nevertheless sought an additional and independent means to confirm these values. This was accomplished using ac susceptibility data collected on microcrystalline samples in a 3.5 G ac field. The in-phase (χ_M') ac susceptibility signal is invaluable for assessing S without any complications from a dc field, and these signals for complexes **1**−**3** at 997 Hz are plotted as $\chi_M'T$ vs T in Figure 9. Extrapolation of the plots to 0 K, from temperatures above ~5 K to avoid the effect of weak intermolecular interactions (dipolar and superexchange), gives values of ~33, ~27, and ~37 cm^3 K mol^{-1} for **1**−**3**, respectively, corresponding to $S = 8$, 7, and 8, respectively, with $g \sim 1.91$, 1.96, and 2.02, in very satisfying agreement with the conclusions from the fits of the dc magnetization data.

(27) (a) Soler, M.; Wernsdorfer, W.; Folting, K.; Pink, M.; Christou, G. *J. Am. Chem. Soc.* **2004**, *126*, 2156. (b) Boskovic, C.; Wernsdorfer, W.; Folting, K.; Huffman, J. C.; Hendrickson, D. N.; Christou, G. *Inorg. Chem.* **2002**, *41*, 5107.

(28) (a) Brechin, E. K.; Sanudo, E. C.; Wernsdorfer, W.; Boskovic, C.; Yoo, J.; Hendrickson, D. N.; Yamaguchi, A.; Ishimoto, H.; Concolino, T. E.; Rheingold, A. L.; Christou, G. *Inorg. Chem.* **2005**, *44*, 502. (b) Sanudo, E. C.; Wernsdorfer, W.; Abboud, K. A.; Christou, G. *Inorg. Chem.* **2004**, *43*, 4137.

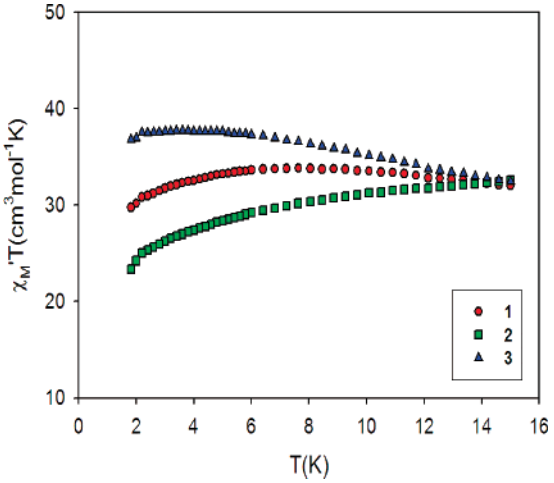

Figure 9. Plots of ac $\chi_M'T$ vs T for complexes **1**·$2H_2O$ (●), **2** (■), and **3**·$5H_2O$ (▲) at 997 Hz.

None of the complexes displayed out-of-phase (χ_M'') ac susceptibility peaks above 1.8 K. There were some very weak signs of the beginning of signals whose peaks would lie well below 1.8 K, and these may correspond to the very small dips in the $\chi_M'T$ plots of Figure 9 at $T < 2$ K. However, it is clear that if any of the complexes **1**−**3** were SMMs, they would at best have very small barriers to magnetization relaxation. In fact, complex **1**, with its combination of $S = 8$ and $D = -0.30$ cm^{-1}, would be predicted to have the largest barrier of the three complexes, with an upper limit (U) of $U = S^2|D| = 19.2$ cm^{-1}. However, the true or effective barrier (U_{eff}) is expected to be significantly less than U, especially given the low symmetry of the molecule, and it is perhaps not surprising that even if **1** were a SMM, it would be one only at very low temperatures (<1 K) and thus not a significant new addition to the family of SMMs.

Conclusions

Deprotonated $edteH_4$ has proven to be a useful new route to a variety of novel Mn_x clusters. It is a hexadentate chelate whose four alcohol groups offer, on deprotonation, the possibility of each bridging to one or more additional Mn atoms and thus fostering the formation of high-nuclearity products. In the present work, we have described the synthesis and characterization of new Mn_8, Mn_{12}, and Mn_{20} products, all with unprecedented structural features and all with significant ground-state spin values of $S = 7$ or 8. The use of $edteH_4$ in a variety of other reactions will undoubtedly lead to many additional and interesting high-nuclearity complexes as this work is extended, and our further efforts along these lines will be reported in due course.

Acknowledgment. We thank the National Science Foundation (CHE-0414555) for support of this work.

Supporting Information Available: X-ray crystallographic data in CIF format for complexes **1**·$2CH_2Cl_2$·MeOH, **2**·6MeCN·$^1/_2H_2O$, and **3**·10MeOH; two-dimensional contour plots of the rms error surfaces vs D and g for the magnetization fits for **2** and **3**·$5H_2O$; space-filling representation of complex **2**. This material is available free of charge via the Internet at http://pubs.acs.org.

IC701971D